Master's Thesis

Characterization of Interaction Between ABBA and NEDD9

Ellinoora Elomaa

2020

Master's Programme in Genetics and Molecular Biosciences

Faculty of Biological and Environmental Sciences

UNIVERSITY OF HELSINKI

HELSINGIN YLIOPISTO
HELSINGFORS UNIVERSITET
UNIVERSITY OF HELSINKI

Faculty	Degree Programme
Faculty of Biological and Environmental Sciences	Master's Programme in Genetics and Molecular Biosciences

Author
Ellinoora Elomaa

Title
Characterization of Interaction Between ABBA and NEDD9

Subject/Study track
Genetics and Genomics

Level	Month and year	Number of pages
Master's thesis	April 2020	41

Abstract

The human cerebral cortex is characteristically large and folded, which can be majorly attributed to the high number and variety of neural progenitors during embryonic development. Radial glial cells are essential neural progenitors during neurogenesis. In addition to giving rise to new cell types, they also provide scaffold for migrating newborn neurons. Radial glia are known to portray peculiar characteristics in their cell division process, including unique migratory behavior as well as specifically regulated cleavage furrow orientation. While these processes of radial glial division have been studied extensively, the underlying molecular mechanisms are still largely unknown.

ABBA (actin-bundling protein with BAIAP2 homology) and NEDD9 (neural precursor cell expressed, developmentally downregulated 9) are proteins, which are both known to be expressed in certain radial glia progenitors during embryonic development, while they are mainly absent in neurons. ABBA has a defined role of regulating plasma membrane deformation and actin polymerization in radial glia, while NEDD9 expression levels are a known factor in the correct progression from mitosis to cytokinesis. An interaction between ABBA and NEDD9 has previously been identified in a yeast two-hybrid screen done for the embryonic mouse brain.

The aim of this thesis was to validate the interaction between ABBA and NEDD9 biochemically. First, their interaction was evaluated by doing co-immunoprecipitation assays on the endogenous proteins from C6 cells. The second approach was to test, whether their interaction is directly mediated by the N-terminal SH3-domain of NEDD9 and the proline-rich C-terminal portion of ABBA. This was done by doing biochemical binding assays using purified proteins and domains of interest. While co-immunoprecipitation of the two proteins gave results indicating an interaction, I could show that there is no direct binding between NEDD9 SH3-domain and ABBA, suggesting that the interaction might require other domains or be indirect. Together, these results provide valuable information that will help characterize what roles of ABBA and NEDD9 play in cortical development and beyond.

Keywords
ABBA, NEDD9, radial glial cells, protein interactions

Supervisor or supervisors
Group leader, Asst. Prof. Juha Saarikangas (Ph.D.)

Where deposited
HELDA - Digital Repository of the University of Helsinki

Additional information

Tiedekunta	Koulutusohjelma
Bio- ja ympäristötieteellinen tiedekunta	Genetiikan ja molekulaaristen biotieteiden maisteriohjelma

Tekijä
Ellinoora Elomaa

Työn nimi
ABBA- ja NEDD9-proteiinien välisen vuorovaikutuksen karakterisointi

Oppiaine/Opintosuunta
Genetiikan ja genomiikan opintosuunta

Työn laji	Aika	Sivumäärä
Maisterintutkielma	Huhtikuu 2020	41

Tiivistelmä

Ihmisen aivokuoren merkittäviä ominaisuuksia ovat sen suuri koko ja poimuttuneisuus. Nämä piirteet ovat laajalti alkiovaiheen kehityksen aikaisten hermokantasolujen korkean määrän sekä monimuotoisuuden ansiota. Radiaaligliasolut ovat erityisen suuressa roolissa alkion neurogeneesin aikana, sillä ne tuottavat useita eri solutyyppejä sekä toimivat mekaanisena tukena vastasyntyneille hermosoluille, jotka vaeltavat aivokuoren kehityksen aikana kohti lopullista sijaintiaan. Näille soluille tyypillisiä ominaispiirteitä ovat niiden jakautumiseen liittyvät ainutlaatuiset prosessit, kuten sooman migraatio solusyklin eri vaiheiden aikana sekä jakautumistason tarkka säätely. Vaikka näiden solujen jakautumisprosesseja on tutkittu melko laajalti, niiden taustalla vaikuttavat molekyylitason mekanismit ovat vielä suurelta osin tuntemattomia.

ABBA ja NEDD9 ovat proteiineja, joiden on todettu esiintyvän radiaaligliasoluissa alkionkehityksen aikana. ABBA toimii säätelijänä solukalvon dynaamisissa muutoksissa sekä aktiinin polymerisaatiossa radiaaligliasoluissa, kun taas NEDD9-ekspressiotasoilla on osoitettu olevan suora vaikutus solujen kykyyn edetä mitoosista sytokineesiin. ABBA- ja NEDD9-proteiinien välillä on aiemmin todettu vuorovaikutus Y2H (yeast two-hybrid) -seulonnassa.

Tämän pro gradu -tutkielman tavoitteena oli vahvistaa ABBA- ja NEDD9-proteiinien välinen vuorovaikutus biokemiallisesti. Ensin niiden vuorovaikutusta arvioitiin ko-immunopresipitaatiolla, joissa käytettiin C6-glioomasolujen endogeenisia proteiineja. Toinen lähestymistapa oli testata, onko näiden proteiinien välillä kyseessä välitön interaktio NEDD9:n N-terminaalisen SH3-domeenin sekä ABBA:n proliinirikkaan C-terminaalisen osan välillä. Tämä hypoteesi testattiin käyttämällä puhdistettuja proteiineja sekä domeeneja biokemiallisissa sitoutumisanalyyseissä. Vaikka ko-immunopresipitaatio-analyyseissä ilmeni selkeä vuorovaikutus, kykenin osoittamaan, ettei NEDD9 SH3-domeenin ja ABBA:n välillä ole suoraa sitoutumista. Tämä viittaa siihen, että vuorovaikutus voi vaatia muita domeeneja tai olla epäsuora. Nämä tulokset tarjoavat uutta tietoa, joka auttaa karakterisoimaan ABBA:n ja NEDD9:n biologista merkityksistä aivokuoren kehityksessä sekä muissa konteksteissa.

Avainsanat
ABBA, NEDD9, radiaaligliasolut, proteiinien välinen vuorovaikutus

Ohjaaja tai ohjaajat
Ryhmänohjaaja, apulaisprofessori Juha Saarikangas (FT)

Säilytyspaikka
HELDA - Helsingin yliopiston digitaalinen arkisto

Muita tietoja

Table of Contents

Abbreviations

ABBA	Actin-bundling protein with BAIAP2 homology
BAR	Bin-Amphiphysin-Rvs
CAS	Crk-associated substrate-related
IPC	Intermediate progenitor cell
K_D	Equilibrium dissociation constant
MCD	Malformation of cortical development
msfGFP	Monomeric superfolder green fluorescent protein
MST	MicroScale Thermophoresis
NEDD9	Neural precursor cell expressed, developmentally downregulated 9
NTA	Nitrilotriacetic acid
oRGC	Outer radial glial cell
oSVZ	Outer subventricular zone
RGC	Radial glial cell
SPR	Surface plasmon resonance
SH3	Src Homology 3 domain
vRGC	Ventricular radial glial cell
WH2	WASP homology 2 domain

1. Introduction

1.1. Cortical development and radial glial cells

The expanded size and folded surface area of the human neocortex enables more advanced cognitive activity compared to other mammalian species. This characteristic of the human brain can be attributed to the evolutionary increase in the number and proliferative potential of neural progenitors during embryonic development (Borrell, 2019; Lui et al., 2011). A specific type of neural progenitors known as radial glial cells (RGCs) are responsible for two main functions during cortical development: giving rise to new cells and guiding the migration of newborn neurons through scaffolding (Chou et al., 2018). The different functions of RGCs depend on their unique structure and apico-basolateral polarity. RGCs form a particular type of polarized, pseudostratified epithelium which lines the ventricular wall during cortical development (Chou et al., 2018).

RGCs are classified into ventricular RGCs (vRGCs; also known as apical RGCs) and outer RGCs (oRGCs; also known as basal RGCs). Neurogenesis begins as neuroepithelial cells, which mainly divide symmetrically, transition into RGCs, which can undergo asymmetric divisions in addition to self-renewal (Chou et al., 2018). vRGCs emerge first, and during early development they populate the ventricular zone through symmetric divisions to increase the initial vRGC progenitor population (LaMonica et al., 2013; Ostrem et al., 2016; Figure 1). vRGCs are the primary cortical progenitors and produce neurons through direct neurogenesis by dividing asymmetrically (Borrell, 2019). vRGC divisions can either be vertical (cleavage furrow is perpendicular to the ventricular surface), horizontal (cleavage furrow is parallel to the ventricular surface) or oblique (LaMonica et al., 2013). Vertical vRGC divisions can either be a source of self-renewal or give rise to intermediate progenitor cells (IPCs), while later in neurogenesis horizontal vRGC divisions produce oRGCs (LaMonica et al., 2013). oRGCs are also born from vRGCs that delaminate from the ventricular surface (Ostrem et al., 2016). Both IPCs and oRGCs can also produce cortical neurons through a process known as indirect neurogenesis, which enables a higher level of cortical expansion (Borrell, 2019; Hansen et al., 2010).

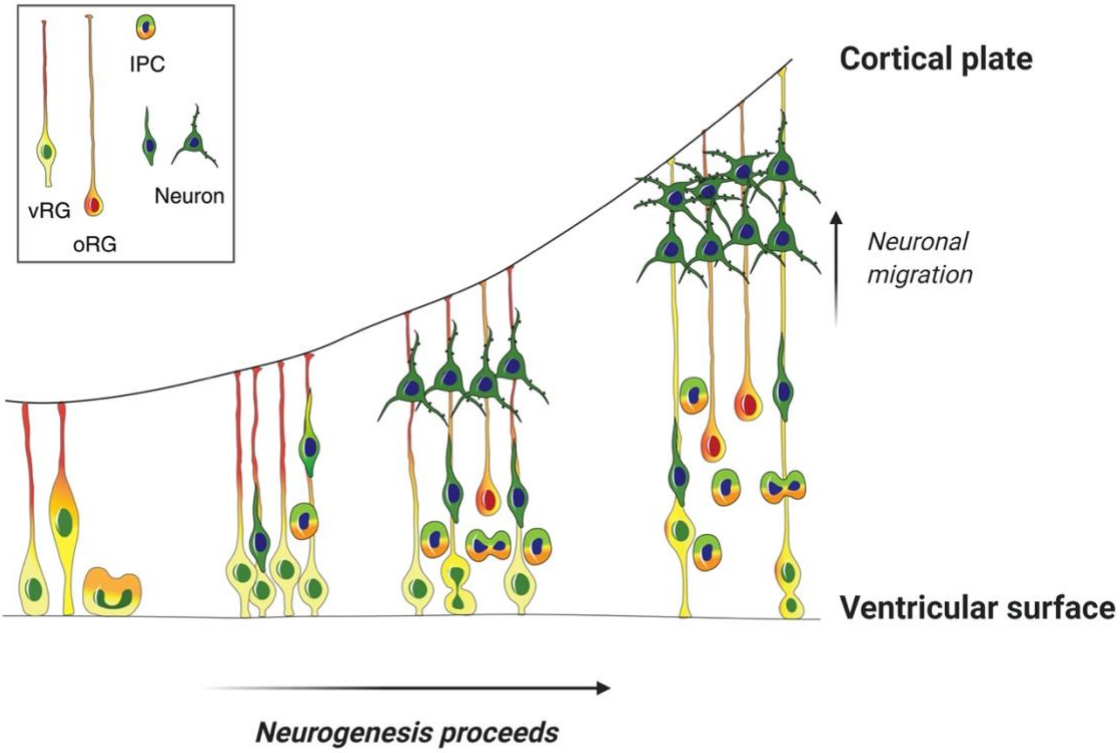

Figure 1. Different types of radial glial cells throughout cortical development. Ventricular radial glia (vRG) are the first cell type to emerge at the beginning of neurogenesis, and they mainly divide symmetrically for self-renewal during early cortical development. Outer radial glia (oRG), intermediate progenitor cells (IPCs) and neurons emerge from asymmetric divisions later, as neurogenesis proceeds. The migration of newborn neurons towards the cortical plate is guided with a scaffold provided by the basal processes of radial glia. The image is modified from Ostrem et al., 2016.

The soma of a vRGC is located close to the ventricular surface and it has contact with both the ventricular surface through its apical domain, as well as the pial surface through an extensive membrane protrusion known as the basal fibre (Chou et al., 2017; Ostrem et al., 2016; Figure 1). Inheritance of these apical and basal processes has a significant role in cell fate determination of vRGC divisions (Chou et al., 2017; LaMonica et al., 2013). oRGCs have a basal fibre similar to vRGCs, but they lack contact with the ventricular surface (Ostrem et al., 2016). The basal fibres of RGCs extend across the developing cortical layers towards the pial surface, and provide a scaffold for neuronal migration (Chou et al., 2017). After neurons and IPCs are born from vRGCs at the ventricular surface, they must delaminate and migrate towards the cortical plate and their final locations (Borrell, 2019; Figure 1). The long basal processes of vRGCs could also provide a

mechanism for the regulation of neural progenitor proliferation by transporting certain mRNAs to the pial surface for local translation (Borrell, 2019).

While oRGCs share some similarities with vRGCs in their molecular components and morphology, they have unique characteristics and roles in cortical development. The majority of oRGC divisions lead to self-renewal through horizontal division, while only a small portion of divisions generate IPCs (LaMonica et al., 2013; Ostrem et al., 2016). This characteristic could be explained by oRGCs being transit-amplifying cells, which means that they undergo many rounds of self-renewal before differentiation to IPCs (Ostrem et al., 2016). oRGCs populate the outer subventricular zone (oSVZ) during development and their divisions lead to the expansion of the oSVZ. This attributes to upper layer neurogenesis and it is seen as a significant process in primate neocortex development (Lui et al., 2011; Ostrem et al., 2016). A higher proliferation rate of both IPCs and oRGCs has been linked to species with a large and folded cortex (Borrell, 2019).

Both vRGCs and oRGCs undergo unique migratory behaviors throughout their cell cycles. vRGCs go through a process known as interkinetic nuclear migration, where their nuclei migrate away from the ventricular surface along the basal fibre after mitosis (Chou et al., 2017). The nuclei then migrate back before the start of a new cell cycle. oRGCs undergo a similar process known as mitotic somal translocation, where their soma moves towards the cortical plate before cell division (Ostrem et al., 2016). Although these processes seem very similar, they appear to have distinct underlying molecular mechanisms (Ostrem et al., 2014). Mitotic somal translocation of oRGCs likely contributes to more extensive transit amplification within the oSVZ (Hansen et al., 2010). It may also be a target in some cortical malformations (Ostrem et al., 2014).

At the end of neurogenesis RGCs begin to give rise to oligodendroglial lineage progenitors (Chou et al., 2017). By the time of birth distinct subpopulations of RGCs have shifted to producing ependymal cells while others have transformed into ventricular-subventricular zone type B1 cells (Beattie and Hippenmeyer, 2017). Type B1 cells are the prominent stem cell progenitors during adult neurogenesis (Beattie and Hippenmeyer, 2017). After birth most RGCs have transitioned into astrocytes and adult neural stem cells (Chou et al., 2017). Although RGCs seem to mostly disappear after birth, it has been found that radial glia fibres in neonatal mice provide scaffold for the migration of neuroblasts toward the injured area of the cortex (Jinnou et al., 2018).

Defects in cortical developmental processes can lead to different types of malformations of the cerebral cortex. Malformations of cortical development (MCDs) can be classified into subgroups based on the cellular mechanisms underlying the malformation, and how early in development the process is disrupted. For example, microcephalies and overgrowth disorders are classified into a group of malformations that follow abnormal cell proliferation or apoptosis (Desikan and Barkovich, 2016). Other subgroups of these disorders are malformations following abnormal cell migration (Group II) and malformations following abnormal postmigrational development (Group III). Defects in RGC functions are often involved in these underlying mechanisms (Desikan and Barkovich, 2016). MCDs commonly cause neurodevelopmental delay and drug-resistant early-onset epilepsy (Reghunath and Ghasi, 2020). Understanding and investigating the molecular mechanisms involved in cortical development provides valuable insight for these disorders as well.

1.2. ABBA

ABBA (actin-bundling protein with BAIAP2 homology) was initially identified as a member of the IRSp53-MIM protein family (Saarikangas et al., 2008), which are classified as members of the BAR (Bin, Amphiphysin, Rvs) domain superfamily of proteins (Stanishneva-Konovalova et al., 2016; Zhao et al., 2011). Saarikangas and others (2008) discovered that ABBA is abundant in radial glial cells during embryonic development, while it is absent in embryonic neurons. In radial-glia-like C6-R cells endogenous ABBA is enriched at the interface between the cortical actin cytoskeleton and the plasma membrane, and it regulates plasma membrane deformation and actin polymerization during protrusive events in these cells (Saarikangas et al., 2008).

While ABBA has not been extensively studied outside the context of radial glial cells, it has been shown that ectopic expression of ABBA induces membrane ruffling and cell spreading in mouse fibroblasts, which is likely mediated by an interaction between ABBA and Rac1 (Zeng et al., 2013; Zheng et al., 2010). Additionally, Chatzi and others (2019) recently found that ABBA expression was highly induced in activated hippocampal dentate granule cells after a single period of short-term exercise in adult mice. They hypothesized that ABBA might be involved in the induction and rearrangement of synapses in postsynaptic dendrites (Chatzi et al., 2019).

Members of the BAR domain family function as regulators of membrane rearrangements in eukaryotes. They are able to generate and detect local membrane curvatures, as well as recruit other cytosolic proteins to specific cell sites and affect actin dynamics directly or indirectly (Stanishneva-Konovalova et al., 2016). In general, BAR domains bind through their positively charged amino acids to negatively charged lipids in membranes (Stanishneva-Konovalova et al., 2016). BAR domains are divided into subgroups based on their phylogenetic and structural characteristics: BAR/N-BAR, F-BAR, and I-BAR groups. Even within these subfamilies, there are distinctive differences between domain functions (Saarikangas et al., 2009).

ABBA is specifically a part of the I-BAR (Inverse BAR) group. While classical and F-BAR domains induce membrane invaginations (positive membrane curvature), I-BAR domains induce membrane protrusions to the opposite direction (negative membrane curvature) (Zhao et al., 2011). This is due to I-BAR domains binding specifically to the inner surface of membrane tubules (Saarikangas et al., 2009) as well as their geometry being convex- rather than concave-shaped like other BAR domains (Zhao et al., 2011). Proteins of the I-BAR group can be further divided into the MIM-like subset (including ABBA and MIM) and the IRSp53 (insulin receptor tyrosine kinase substrate p53) subset (including IRSp53, IRTKS and FLJ22582). ABBA and MIM share a very similar domain structure (Stanishneva-Konovalova et al., 2016; Zhao et al., 2011).

In addition to its N-terminal I-BAR domain, ABBA also has a serine-rich region, three proline-rich regions, a leucine zipper motif and a C-terminal WASP (Wiscott-Aldrich Syndrome Protein) Homology 2 domain (WH2) (Figure 2). The WH2 domain of ABBA binds ATP-actin monomers with a high affinity (Saarikangas et al., 2008).

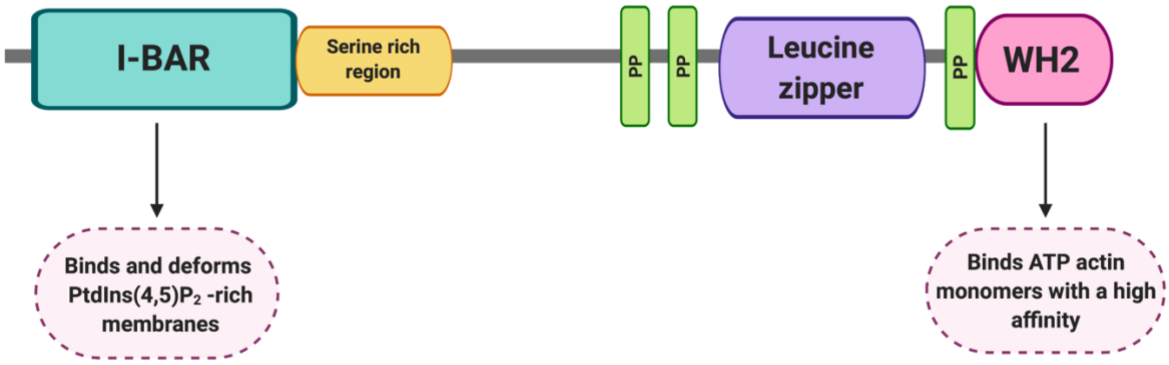

Figure 2. Domain structure of ABBA; I-BAR = Inverse BAR domain; PP = polyproline motif; PtdIns(4,5)P_2 = phosphatidylinositol-4,5-biphosphate; WH2 = WASP (Wiscott-Aldrich Syndrome Protein) Homology 2 domain.

1.3. NEDD9

NEDD9 (neural precursor cell expressed, developmentally downregulated 9) was identified by Kumar and others (1992) as a gene that was highly expressed in the embryonic mouse brain and developmentally downregulated. It is also known as the Human enhancer of filamentation 1 (HEF1) or Crk-associated substrate-related protein lymphocyte type (Cas-L) (Zhang and Wu, 2015). NEDD9 has been shown to be expressed in certain radial glia progenitors during embryonic development, while it is absent in neuronally committed cells (Aquino et al., 2008). In 2009, Aquino and others demonstrated a role for NEDD9 in neural crest cell migration. Vogel and others (2010) identified NEDD9 as an important downstream signaling element in Tgfβ-induced neuronal differentiation in cortical and hippocampal mouse progenitors, suggesting it also having a role in cell fate regulation.

Although NEDD9 expression seems to be limited in the adult brain, Sasaki and others (2005) found that it was re-upregulated in the hippocampal and cortical neurons of rats after transient global ischemia. Additionally, Knutson and others (2015) demonstrated that NEDD9 is expressed in the cerebral cortex and hippocampus of adult mice, and it could possibly have a role dendritic spine maintenance.

NEDD9 is a member of the Crk-associated substrates (CAS) family of proteins, which also includes p130Cas and Efs/Sin. CAS proteins are involved in a variety of major cellular processes, including cell cycle, apoptosis, migration and proliferation (Tikhmyanova et al., 2010; Zhang and Wu, 2015). In general, CAS proteins function as scaffolds for a large number of different partners, and therefore intermediate various signaling pathways. While other CAS family members appear to be expressed in most cell and tissue types, NEDD9 expression varies notably (Pugacheva and Golemis, 2006; Tikhmyanova et al., 2010). CAS proteins are associated with focal adhesions, where they localize during interphase (Pugacheva and Golemis, 2006).

CAS proteins share a conserved structure containing four major domains (Tikhmyanova et al., 2010; Figure 3). In NEDD9 the amino-terminal Src homology 3 (SH3) domain is encoded by amino acids 10-65 (Zhang and Wu, 2015). The SH3-domain is known to mediate binding with polyproline motifs (Kurochkina and Guha, 2013; Ohba et al., 1998). The substrate domain, encoded by amino acids 90-350, contains YxxP motifs which act as binding sites for SH2 domains. Amino acids 350-650 contain a serine rich region, which forms a four-helix bundle and likely has a protein binding function. Finally, the carboxy-terminus of NEDD9 is highly conserved in all CAS proteins and binds to proteins with helix-loop-helix domains (Tikhmyanova et al., 2010; Zhang and Wu, 2015). The C-terminus of NEDD9 allows both homodimerization and heterodimerization (Tikhmyanova et al., 2010).

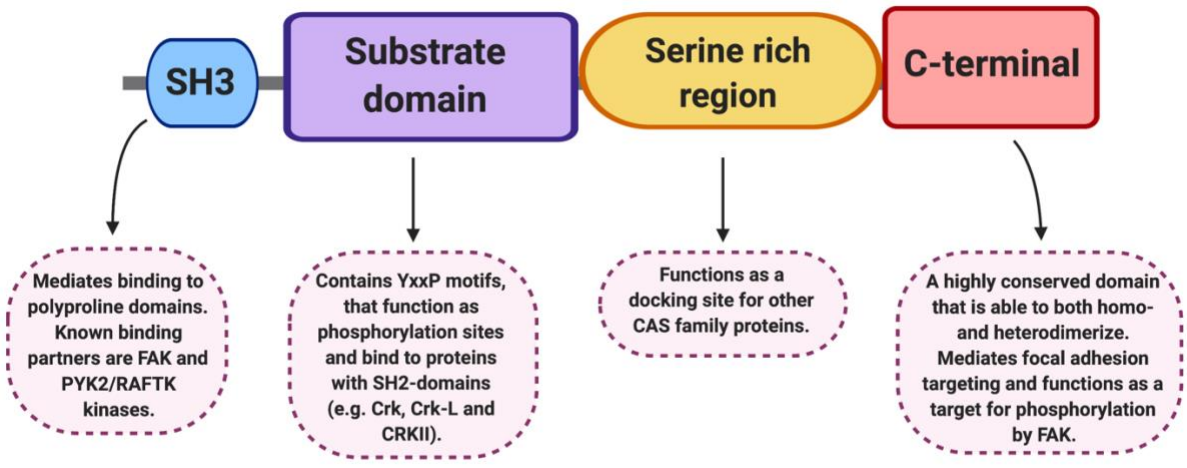

Figure 3. Domain structure of NEDD9 and significant known functions of each domain; SH3 = Src Homology 3 domain

Similarly to all CAS family proteins, NEDD9 expression is regulated mainly through phosphorylation and proteolytic degradation (Tikhmyanova et al., 2010; Zhang and Wu, 2015). Levels of NEDD9 expression are regulated depending on the cell cycle. NEDD9 expression is highest during the G2-phase and mitosis, and lowest during G1-phase (Pugacheva and Golemis, 2005). At the G2-phase NEDD9 localizes at the centrosome, then migrates along the mitotic spindle as mitosis progresses, and finally by cytokinesis it is localized and degraded at the midbody (Pugacheva and Golemis, 2005). Dadke and others (2006) showed that abnormal levels of NEDD9 expression cause defects in cell cycle progression. They found that while NEDD9 overexpression inhibits cells from progressing through cytokinesis, its depletion results in defects earlier during mitosis. This can be explained by the regulation of RhoA by NEDD9, since RhoA inactivation is needed for cytokinesis (Dadke et al., 2006).

NEDD9 and the other CAS proteins have been extensively studied in the context of their role in cancer metastasis (Tikhmyanova et al., 2010). Altered NEDD9 expression levels have been identified as a significant contributor for tumor aggressiveness, metastatic potential and resistance to treatment in many different types of cancer (Shagisultanova et al., 2015). Thus, NEDD9 is regarded as a possible target for cancer therapy.

1.4. Motives for investigating the interaction of ABBA and NEDD9

An interaction between ABBA and NEDD9 has previously been identified in a yeast two-hybrid screen, where full length mouse ABBA-1 (amino acids 1-715) was used as a bait, and interacting partners were screened from a mouse embryo brain prey library (Hybrigenics). According to the Hybrigenics statistical confidence score, known as the Predicted Biological Score (PBS), the interaction between ABBA and NEDD9 was ranked a level C, which means there is good confidence in the interaction based on local and global technical parameters. The interaction was mapped to the N-terminal region of NEDD9, which contains the SH3-domain (Figure 3). This domain is generally known for interacting with proline rich regions. ABBA contains several putative proline rich regions of unknown function (Saarikangas et al. 2008; Figure 2). So far, one missense patient mutation resulting in change of amino acid 597 from threonine to methionine has been published

and linked to a brain dysfunction (Alazami et al., 2015). Interestingly, this mutation is situated in one of the proline-rich regions of the human ABBA.

The biological roles of ABBA and NEDD9 in the context of brain development are not well known, but at the time of starting this thesis, data available at the International Mouse Phenotyping Consortium website indicated that ABBA knockout mice display decreased primary motor cortex size. Different types of malformations of cortical development are a characteristic phenotype of radial glial dysfunction (Desikan and Barkovich, 2016). Therefore, since both ABBA and NEDD9 are strongly expressed in radial glial cells (Aquino et al., 2008; Saarikangas et al., 2008), I hypothesized that these proteins might interact in these progenitor cells and regulate important aspects of brain development .

2. Aims

From these data we hypothesized that ABBA and NEDD9 interact physically in radial glial cells and are important for proper cortical development. The aim of my thesis was to try to validate the interaction between ABBA and NEDD9 biochemically. First, I wanted to validate their interaction by doing co-immunoprecipitation assays on the endogenous proteins from C6 glioma cells. The second aim was to test whether there is a direct interaction between the SH3-domain of NEDD9 and ABBA. I investigated this by doing biochemical binding assays using purified proteins and domains of interest.

3. Materials and methods

3.1. Cell culture maintenance and cell lysis

The C6 glioma cell line was maintained in Dulbecco's modified eagle's medium (DMEM; pH 7,4) supplemented with 10 % fetal bovine serum (Gibco) and 1 % (50 units/ml) penicillin streptomycin (Gibco). The cells were grown in a ThermoForma Steri Cycle CO_2 incubator at +37 °C with 5 % CO_2.

The cells were lysed at a 100 % confluency using a lysis buffer containing: 20 mM Tris-HCl (pH 8.0), 137 mM NaCl, 10 % glycerol, 1 % Triton X-100, 2 mM EDTA and PBS added until final volume. Protease inhibitors were added to the lysis buffer immediately before use: 50 µg/ml PMSF (Roche) and cOmplete Mini EDTA-free Protease Inhibitor Cocktail (Roche) tablets (1 tablet/10 ml of lysis buffer). Before lysis the cells were placed on ice and washed with cold PBS. Lysis buffer was added on the cells (1 ml per 100 mm dish) and the cell suspension was collected. The cell suspension was incubated for 30 min at +4 °C in agitation and then centrifuged (20 min, 12000 rpm, +4 °C). Cleared C6 lysate (supernatant) was collected and the pellet discarded.

Protein concentrations of the cell lysates were determined according to the manufacturer's instructions with the Pierce BCA Protein Assay Kit (Thermo Scientific). C6 cell lysates for co-immunoprecipitation experiments were frozen with liquid nitrogen and stored in -70 °C.

3.2. Co-Immunoprecipitation and Western blot analysis

For the co-immunoprecipitation of endogenous ABBA and NEDD9, ABBA was pulled down from the C6 cell lysate with anti-ABBA primary antibody and Pierce Protein A/G Magnetic Beads (Thermo Scientific). The pulled down sample was then eluted from the beads and analyzed with Western blot to see if NEDD9 had been indirectly captured with ABBA. The primary and secondary antibodies used in the experiments are presented in Table 1.

Table 1. Antibodies used in co-immunoprecipitation and Western blot experiments

Type	Name	Class	Manufacturer or source
Primary	Mouse anti-HEF1	Monoclonal	abcam
Primary	Rabbit anti-ABBA	Polyclonal	Generated by Saarikangas et al. (2008)
Secondary	Rabbit anti-mouse IgG (HRP-conjugated)	Polyclonal	Invitrogen
Secondary	Goat anti-rabbit IgG (HRP-conjugated)	Recombinant polyclonal	Invitrogen

The antigen sample (C6 cell lysate) containing ~1000 µg of protein and 20 µl of anti-ABBA primary antibody were combined and incubated overnight (O/N) in +4 °C with mixing. Before use, 25 µl (0,25 mg) of magnetic beads were washed with a wash buffer containing: TBS and 0,05 % Tween-20 (Sigma). For every wash step the beads were gently mixed and collected with a magnetic stand. The antigen-antibody mixture was combined with the pre-washed beads and incubated at room temperature (RT) for 1 hour with mixing. The beads were collected and the flow-through was saved for later analysis. Pre-washed magnetic beads combined with the antigen sample without antibody were used as a negative control.

The beads were washed 3 x with the wash buffer and 1 x with purified water before elution. Elution was either done by A) adding 30 µl of SDS-PAGE reducing sample buffer to the tube and incubating the beads at RT for 10 min with mixing before separation, or B) doing a low pH elution by adding 50 µl of elution buffer (0,1 M glycine; pH 2,0), incubating the beads at RT for 10 min with mixing, and finally adding 7,5 µl of neutralization buffer (1 M Tris; pH 7,5-9) before magnetically separating the beads. The differences resulting from these two methods are shown and discussed further in Results (Chapter 4.1.).

Original C6 lysate, flow-through sample, negative control and eluted sample were analyzed with Western blotting. Samples were heat shocked for 5 min at +100 °C and cooled down on ice before loading on a 4-20 % Mini-PROTEAN TGX Gel (Bio-Rad). The gels were run at 150 V until the front reached the marked line. Blotting was done using the Trans-Blot Turbo Mini PVDF Transfer Packs

and Transfer System (Bio-Rad). Blotted membranes were blocked with 5% milk solution in TBST (TBS with 0,1 % Tween-20) for 1 hour on a rocking platform in RT. The membrane was then incubated O/N in +4 °C on a rocking platform with a 1:1000 dilution of anti-NEDD9 primary antibody in 5 % milk in TBST. The membrane was then rinsed 1 x and washed 3 x 5 min with TBST. Membrane was incubated in 1:1000 dilution of secondary antibody in 5% milk TBST for 1h on a rocking platform in RT, rinsed 1 x and washed 2 x 5 min with TBST. HRP detection of secondary antibodies was done according to the manufacturer's instructions with the Pierce ECL Western Blotting Substrate (Thermo Scientific). Blotted membranes were imaged with UVP.

3.3. Plasmid construction

The ABBA C-terminal fragment corresponding to residues 274-715 was previously cloned into the pHAT1 vector (Saarikangas et al. 2008) and obtained from the Lappalainen group.

A DNA-fragment corresponding to the SH3-domain of NEDD9 was amplified by PCR and cloned into the pBAT4-msfGFP-HsTpm2 vector (also obtained from the Lappalainen group). All primers used in plasmid constructions are listed in Table 2. The vector was linearized using primers 361 and 362, which exclude the TPM2 gene from the vector. The SH3-domain was extracted with primers 359 and 360 which contained overlapping regions of the vector.

To create the negative control for the biochemical binding assays, a His-tagged msfGFP was also purified (without the SH3-domain). For this, the original vector was linearized with primers 361 and 362 and the TPM2-gene was excluded.

Finally, for cloning msfGFP-constructs with a TEV-protease site (Glu-Asn-Leu-Tyr-Phe-Gln-Ser) in order to remove the 6xHis affinity tag after purification, primers 436 and 437 were used to linearize the vector, and insert the protease site between the 6xHis-tag and msfGFP or msfGFP-SH3.

Table 2. Primers used in plasmid constructions

Primer ID and name	Sequence	Description
OJS00359 NEDD9_SH3_HR_frw	5’- TCT CGG CAT GGA CGA GCT GTA CAA GGG ATC CAT GGC TTC TAT GGC AAG GGC CTT ATA TGA CAA TG -3’	Forward primer designed to replace Tpm2 with the SH3-domain of NEDD9 in vector pBAT4-msfGFP-HsTpm2 by homologous recombination. Contains SH3 sequence from NEDD9 and overhangs of plasmid PJS0235.
OJS00360 NEDD9_SH3_HR_rev	5’- CAA GCT TAT GCA TGC GGC CGC ATC TAG AGG GCC CGG ATC CTC ACA GAA GCT TCA CCC GGT TGC C -3’	Reverse primer designed to replace Tpm2 with the SH3-domain of NEDD9 in vector pBAT4-msfGFP-HsTpm2 by homologous recombination. Contains SH3 sequence (with STOP) from NEDD9 and overhangs of plasmid PJS0235.
OJS00361 pBAT4_delTPM2_frw	5’- TGA GGA TCC GGG CCC TCT AGA TGC -3’	Forward primer for linearizing vector pBAT4-msfGFP-HsTpm2, so that Tpm2 would be excluded from the sequence. Starts with STOP.
OJS00362 pBAT4_delTPM2_rev	5’- AGA AGC CAT GGA TCC CTT GTA CAG C -3’	Reverse primer for linearizing vector pBAT4-msfGFP-HsTpm2 so that Tpm2 would be excluded from the sequence.
OJS00436 pBAT4_TEV_frw	5'-Phosphate - CAG TCA GTG AGC AAG GGC GAG GAG CTG TTC - 3'	Forward primer for linearizing vector pBAT4-msfGFP-HsTpm2 so that a TEV-protease site is inserted into the sequence in the following order: - 6xHis - TEV - msfGFP -
OJS00437 pBAT4_TEV_rev	5'-Phosphate - GAA GTA CAG GTT CTC GTG ATG ATG ATG ATG ATG TGC CAT GGA TAT ATC - 3'	Reverse primer for linearizing vector pBAT4-msfGFP-HsTpm2 so that a TEV-protease site is inserted into the sequence in the following order: - 6xHis - TEV - msfGFP -

Plasmids were purified according to the according to the manufacturer’s instructions with the GeneJET Plasmid Miniprep Kit (Thermo Scientific). All purified plasmids were verified with Sanger sequencing before further use.

3.4. Protein expression and purification

A BL21 strain of *Escherichia coli* was used for high-level expression of all constructs that were then purified from the bacterial cells (purified constructs are listed in Table 3). 2-3 liters of inoculated bacterial culture supplemented with 100 µg/ml ampicillin was grown at +37 °C with shaking at 220 rpm until an OD600-value of 0,6 was reached. Protein expression was induced by adding IPTG (Thermo Scientific) to the culture until a final concentration of 1 mM. The culture was then induced for 5 hours by growing at +37 °C with shaking (220 rpm). After induction the cells were harvested by centrifugation (4000 x g, 20 min). Cell pellets were stored O/N in -80 °C.

The bacterial cells were lysed with a lysis buffer containing: 50 mM Tris, 200 mM NaCl, 10 mM imidazole; pH 7,5. Protease inhibitors were added to the lysis buffer immediately before use: 50 µg/ml PMSF (Roche) and cOmplete Mini EDTA-free Protease Inhibitor Cocktail (Roche) tablets. Lysozyme (Sigma-Aldrich) was added to the lysate (1 mg/ml) and it was incubated for 30 min on ice. The lysate was then sonicated with the Sonifier Cell Disruptor B-30 (Branson) using 30 x 10 s bursts with a 50 s cooling period between each burst. The lysate was then centrifuged (10000 x g, 30 min, +4 °C) to pellet the cellular debris. The cleared lysate (supernatant) was used for further purification.

For every 4 ml of cleared lysate, 1 ml of Ni-NTA SUPERFLOW (Qiagen) was added. The mixture was incubated overnight at +4 °C on a rotary shaker. Next day, the lysate-Ni-NTA mixture was loaded into a column and the flow-through was collected. The column was washed 2 x with 10 ml of wash buffer containing: 50 mM Tris, 200 mM NaCl, 20 mM imidazole; pH 7,5. Bound protein was eluted with elution buffer containing: 50 mM Tris, 200 mM NaCl, 300 mM imidazole; pH 7,5.

The eluted sample was concentrated to a volume of < 2 ml using Amicon Ultra-15 Centrifugal Filter tubes (Millipore) before gel filtration chromatography. The concentrated sample was fractioned with HiLoad Superdex 200 using a buffer containing: 50 mM Tris, 200 mM NaCl; pH 7,5. Absorbance peaks were monitored with a plotter. Fractions within the highest absorbance peaks were collected and analyzed with SDS-PAGE.

Table 3. Purified protein constructs

Name	Size (kDa)
6xHis-ABBA 274-715	47,9
6xHis-msfGFP-SH3	34,5
6xHis-msfGFP (negative control)	28,2
msfGFP-SH3	33,6
msfGFP (negative control)	27,2

3.5. Biochemical binding assays

All biochemical binding assays were done in the Biomolecular Interactions unit at the University of Helsinki. The purified proteins of interest were analyzed with biochemical binding assays to investigate the expected physical interaction between the SH3-domain of NEDD9 and C-terminal ABBA (amino acids 274-715).

For further analyses, a custom peptide representing amino acids 546 to 560 of ABBA (Table 4) was ordered from Thermo Fisher Custom Peptide Synthesis Services. The choice of this specific region is discussed further in Results (Chapter 4.2.). The peptide was dissolved in 50 % (v/v) DMSO/water at a stock concentration of 3,08 mM and stored in -80 °C.

Table 4. Custom peptide representing amino acids 546-560 of ABBA

Name	Sequence	Size	Purity
ABBA 546-560	PIPIRPPIVPVKTPT	1,625 kDa	> 98 %

3.5.1. MicroScale Thermophoresis

MicroScale Thermophoresis (MST) experiments were done using the Monolith NT.115 (NanoTemper Technologies) and MO.Control software (v1.5.3; NanoTemper). In MST, one binding partner (target) needs to be fluorescently labeled and kept at a constant concentration, while the other non-fluorescent partner (ligand) has a varied concentration by serial dilution. Binding is

determined based on differences in thermophoretic movement of bound and unbound molecules within a thermal gradient. Binding induced changes are detected by changes of the fluorescent signal.

In our analyses 6xHis-msfGFP-SH3 and 6xHis-msfGFP were used as fluorescent targets and 6xHis-ABBA as the non-fluorescent ligand. All MST measurements were performed in Standard treated capillaries (NanoTemper) with 100 % excitation power, blue excitation color (465-490 nm), 40 % MST power and a temperature of +22,0 °C. The target concentrations were at kept at a constant 10 nM, and ligand (ABBA) concentration ranged from 0,0167 mM to 5,08 * 10^{-7} mM. Raw data was analyzed with MO.Affinity Analysis software (v2.3; NanoTemper) to plot binding curves and estimate K_D-values for the interactions.

3.5.2. Surface plasmon resonance

Surface plasmon resonance (SPR) experiments were done using the Biacore T100 (Biacore AB). SPR analyses require one partner to be immobilized onto a chip surface. The capture of histidine-tagged proteins was done via nickel (Ni^{2+}) chelation of NTA using a Series S Sensor Chip NTA (GE Healthcare). All solutions used in the experiments (listed in Table 5) were filtered sterile before use.

Table 5. Solutions used in SPR experiments

Solution	Description
Running buffer	50 mM Tris; 200 mM NaCl; pH 7,5
Nickel solution	0,5 mM $NiCl_2$ (Acros Organics) in water
Regeneration solution	350 mM EDTA; pH 8,3
Washing solution	3 mM EDTA

Before the first analysis cycle of each run, the chip surface was conditioned with regeneration solution (1 min pulse). The NTA chip surface was prepared with nickel solution to saturate the NTA (1 min pulse). 6xHis-ABBA (274-715) was used as the histidine-tagged ligand and captured on the NTA chip using an optimized concentration of 1,25 µg/ml, flow rate of 10 µl/min and a contact time of 60 s.

Interaction analysis was done using the msfGFP and msfGFP-SH3 constructs purified with no His-affinity tag (Table 3). An optimized concentration range from 500 nM to 5000 nM was used for the samples. The analytes were injected at a flow rate of 30 µl/min and a contact time of 180 s. Dissociation time of 300 s was used and all regeneration steps were done using 0,35 M EDTA.

4. Results

4.1. Co-immunoprecipitation of endogenous proteins

In order to see if endogenous ABBA and NEDD9 interact in C6 cells, co-immunoprecipitation experiments were done using ABBA as the primary target protein. Presence of NEDD9 (secondary target) was then analyzed from the final eluted samples, to see if it had been pulled down indirectly in the experiment, which would indicate an interaction between the two proteins.

Western blot results are presented for two different optimization attempts of the co-immunoprecipitation experiments with ABBA and NEDD9 (Figure 4). Since endogenous ABBA was used as the bait-protein in the pull-down assays, anti-NEDD9 bands are showcased in the results. Due to the high level of phosphorylation in the regulation of NEDD9 expression, the protein typically shows two bands at around 105,5 kDa and 115 kDa (Zhang and Wu, 2015). Both of these bands can be seen clearly in the original C6 cell lysate sample and the co-immunoprecipitation flow-through sample (which consists of everything that was not pulled down with ABBA) in both attempts.

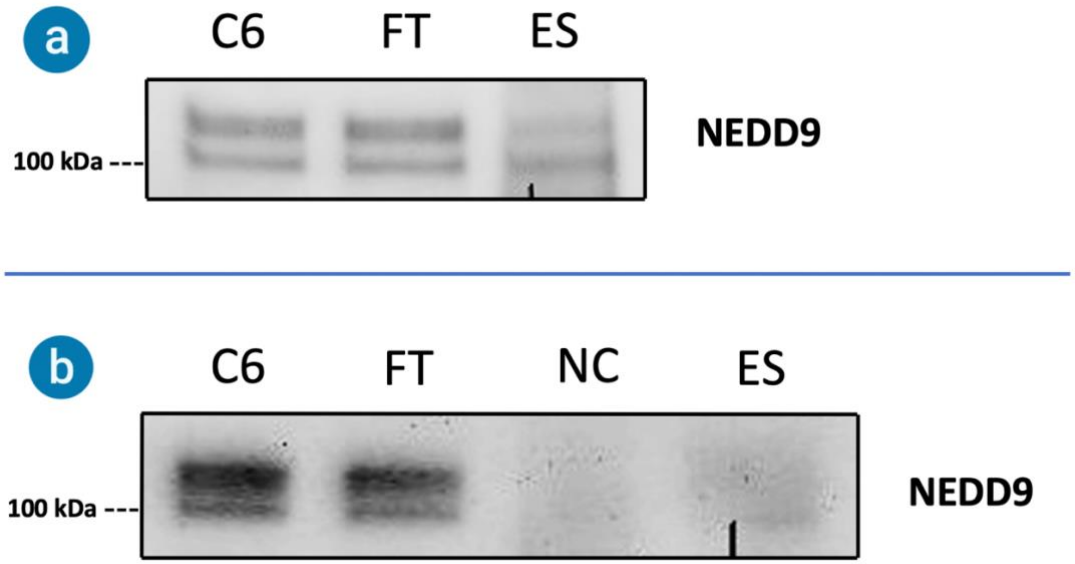

Figure 4. Western blot analysis of co-immunoprecipitation assays for NEDD9 pulldown with endogenous ABBA from C6 cells; C6 = original C6 cell lysate; FT = flow-through sample; NC = negative control; ES = eluted sample.

The first experiment shown (Figure 4a) lacked a negative control. However, the NEDD9 protein bands can be seen much clearer in the eluted sample of the first experiment, in comparison to the second one (Figure 4b), where a negative control was included. This could be explained by different elution methods used in these experiments. In the first experiment (Figure 4a), the final sample was eluted using SDS-PAGE reducing sample buffer, while the second experiment (Figure 4b) was done using low pH elution. Otherwise the two experiments were done using the same protocol and materials (for example primary and secondary antibodies). In total, co-immunoprecipitation involved several optimization steps (altogether seven separate attempts) and based on these results the SDS-PAGE elution gave the best result in preserving the interaction.

Eluted samples from both experiments show a stronger signal for the lower protein band of NEDD9 at around 100 kDa. This indicates, that ABBA binds preferentially to the non- (or less) phosphorylated form of NEDD9. The higher band of 115 kDa represents the hyper-phosphorylated form of NEDD9, which is considered to be the active form of NEDD9 in the context of its ability to bind with various partners.

4.2. Identification of possible SH3-domain interaction sites in the ABBA sequence

Based on the previously done yeast two-hybrid screen, NEDD9 interacts with ABBA through its N-terminal region, which contains an SH3-domain (Figure 3). Therefore, after testing the interaction with endogenous proteins, I wanted to investigate if the interaction of ABBA and NEDD9 is direct and mediated by the SH3-domain of NEDD9 and the proline-rich region of ABBA.

SH3-domains are known to bind both canonical and non-canonical proline rich regions. Canonical SH3 binding sites usually contain a PxxP-motif with possible flanking residues, which can contribute towards binding. These consensus sequences are generally divided into two main classes: class I ligands contain the sequence RXLPPXP, while class II ligands bind in the opposite orientation with the sequence XPPLPXR (Kurochkina and Guha, 2013).

First, both canonical and non-canonical SH3-domain binding sites were searched for within the proline-rich C-terminal region of ABBA. A possible canonical interaction site was identified within ABBA amino acids 546 to 550, based on the class II consensus (Figure 5; Kurochkina and Guha,

2013). A custom peptide representing these amino acids was ordered (Table 4) and used as a possible binding partner in MST and SPR assays with the msfGFP-constructs.

Figure 5. Possible SH3-domain interaction site was identified in the ABBA sequence (amino acids 546-550) based on the canonical class II consensus. A) Protein sequence alignment of mouse (*Mus musculus*) and human (*Homo sapiens*) ABBA. Proline-rich motifs are shown within the dashed red boxes, and the identified consensus sequence within the black box B) Class II consensus sequence represented in the ABBA sequence. The symbol ϕ (Phi) represents a hydrophobic amino acid (valine in the ABBA site) and + represents a positively charged amino acid (lysine in the ABBA site). PxxP is known as a minimal consensus target site for SH3-domain binding and it is often surrounded by specific binding enhancing residues.

4.3. Protein purifications

In order to test the direct interaction with biochemical binding assays, protein constructs representing the domains of interest were purified. I decided to directly focus on purifying individual domains and partial constructs, as the expression and purification of large full-length proteins the size of ABBA and NEDD9 is typically difficult and can result in reduced yields of total protein that is more instable than the individual domains. Since my initial plan was to mainly use MicroScale Thermophoresis for binding analyses, one binding partner needed to be a fluorescently tagged construct. Thus, the SH3-domain of NEDD9 was purified as a part of a 6xHis-tagged msfGFP-construct to be used as the fluorescent partner. The C-terminal portion of ABBA was purified as the non-fluorescent partner, as well as the empty msfGFP-construct as a negative control.

Samples were collected at distinct points during the protein expression and purification process of each construct, which were then analyzed in the end with SDS-PAGE (Figure 6). This was done in order to validate a successful purification, and to determine in the case of an unsuccessful attempt, which step in the expression or purification process had failed. Additionally, collected fractions from fast protein liquid chromatography (FPLC) were analyzed independently with SDS-PAGE, to confirm that they indeed contained the purified protein of interest, before pooling the correct fractions into one sample.

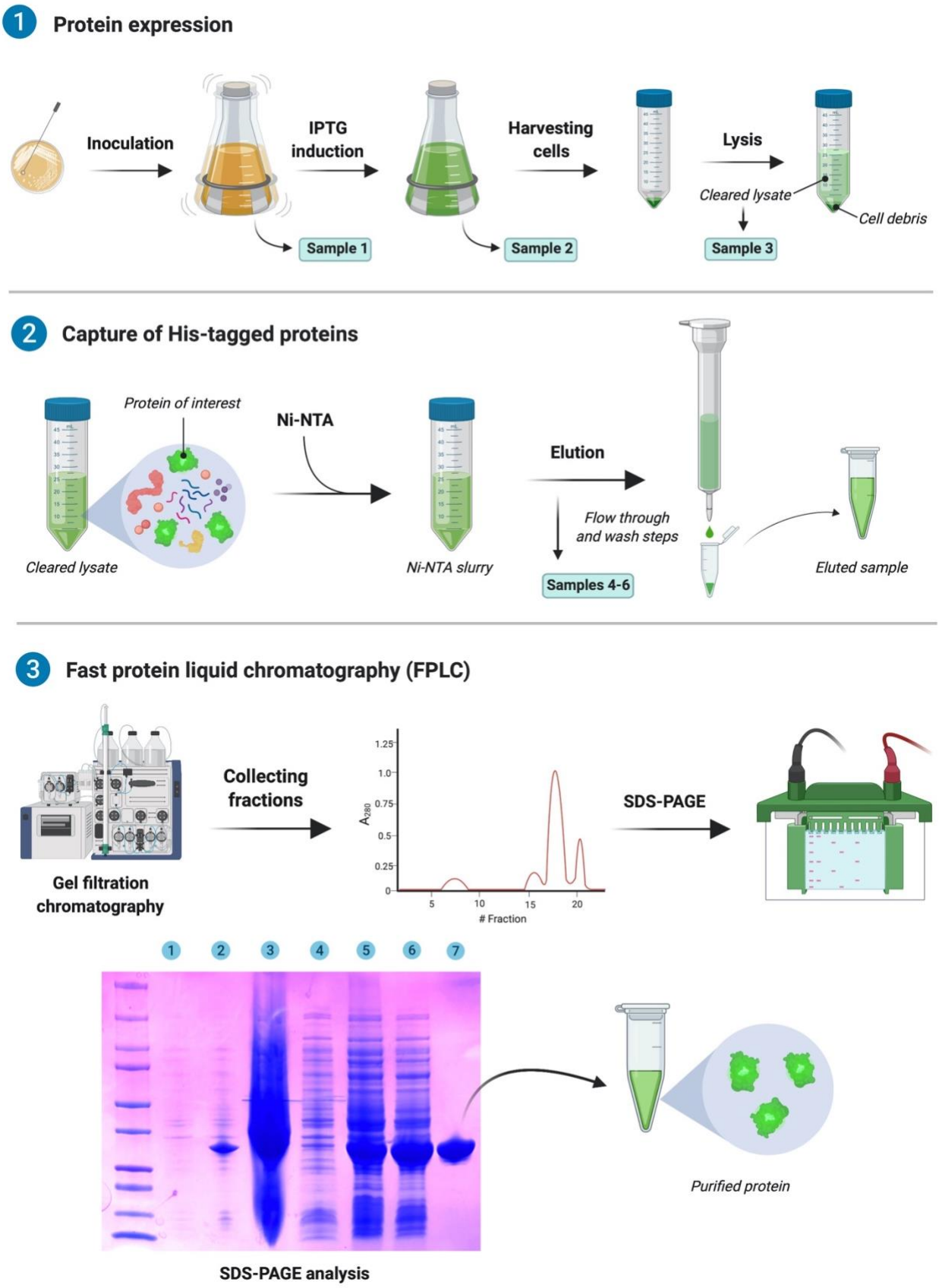

Figure 6. Schematic representation of the protein purification methods. The msfGFP-construct purification is used as an example. Samples taken for final SDS-PAGE analysis at different steps are shown in the figure.

4.4. MicroScale Thermophoresis

MST binding assays were first optimized for ABBA 274-715 as the ligand and msfGFP-SH3 as the fluorescent target. These experimental conditions were repeated for the msfGFP-target, which represents the empty negative control, and in theory should not show any kind of binding with C-terminal ABBA. Surprisingly the results showed very similar quantitative binding affinity in both experiments (Figure 7).

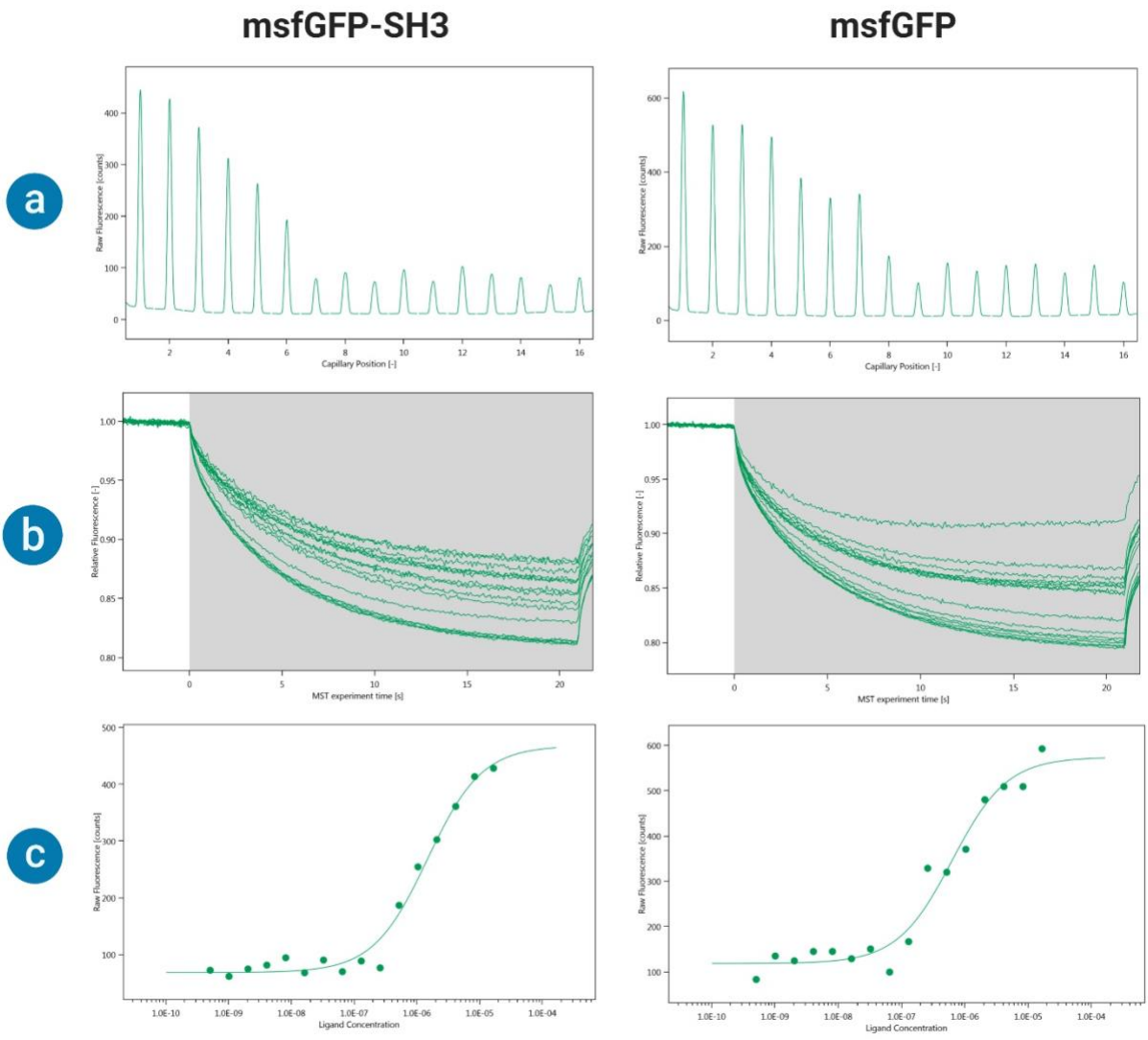

Figure 7. Results from MST binding analyses using ABBA 274-715 as a ligand, and either msfGFP-SH3 or msfGFP as the fluorescent target. A) Capillary scans showing fluorescent target signals in capillaries 1-16. B) MST-traces C) Binding curves were plotted using raw fluorescence values, due to the signal changes.

Capillary scans showed a peculiar pattern in the fluorescence signals (Figure 7a). Since the target concentration is kept at a constant in all 16 capillaries while the ligand (in this case ABBA) concentration changes, fluorescent signal should be consistent in all reactions. However, in both cases the highest signals seem to be induced by higher concentrations of the ligand (capillaries 1 through 6 or 7). This was confirmed not to be caused by a pipetting error by doing several repetitions, and by seeing that addition of a detergent (different concentrations of Tween-20 were tested), the phenomenon disappears. However, the addition of detergent resulted in no binding being detected (data not shown).

Due to these changes in fluorescence, the binding curves were plotted using raw fluorescence counts instead of relative fluorescence (Figure 7c). K_D-values were estimated for both experiments and they are shown in Table 6.

Table 6. Estimated K_D-values from biochemical binding assays

Assay method	Partner 1	Partner 2	K_D-value
MST	ABBA 274-715	msfGFP-SH3	1,472 µM
MST	ABBA 274-715	msfGFP (negative control)	0,629 µM
SPR	ABBA 274-715	msfGFP-SH3	0,905 µM
SPR	ABBA 274-715	msfGFP (negative control)	0,866 µM

4.5. Surface plasmon resonance

Due to MST assays giving quite inconclusive results, I wanted to check binding for the same purified constructs using SPR, where fluorescence is not a contributing factor in binding measurements.

SPR binding assays were first optimized for His-tagged ABBA 274-715 as the immobilized ligand and msfGFP-SH3 (purified without a 6xHis-tag) as the interaction partner that passes over the ligand in solution. These experimental conditions were repeated with using msfGFP as the analyte. Sensograms show the progress of interaction at different analyte concentrations (Figures 8a and 9a). The 1:1 binding model was assumed for ABBA and NEDD9, so interaction affinities could be

determined by measuring steady-state binding levels (Figures 8b and 9b). K_D-values were estimated for both experiments and they are shown in Table 6.

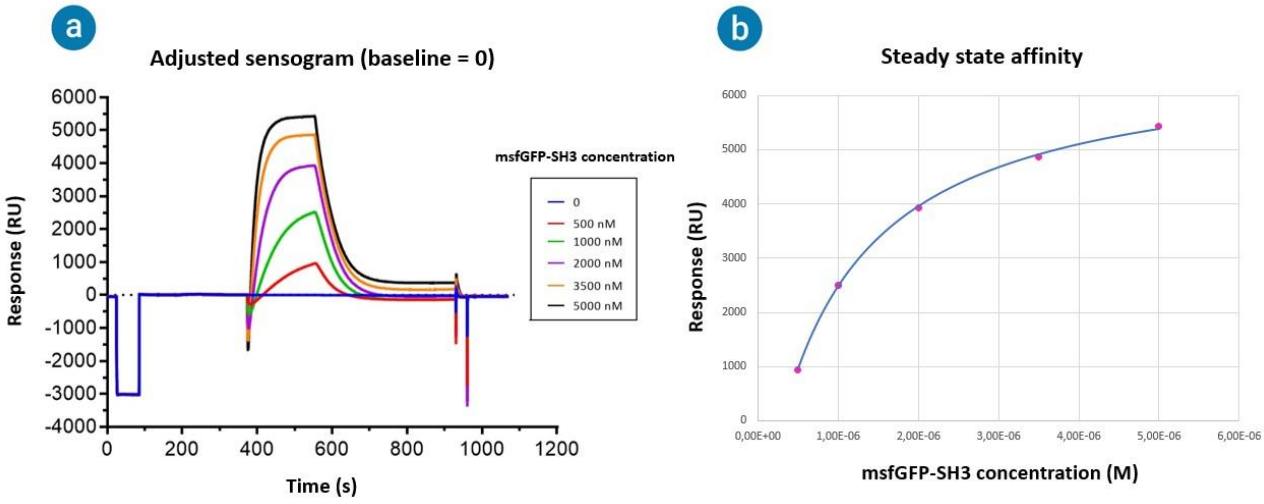

Figure 8. SPR results for binding analysis of ABBA 274-715 and msfGFP-SH3. A) Adjusted sensograms for different concentrations of analyte; B) Steady state affinity; RU = resonance unit

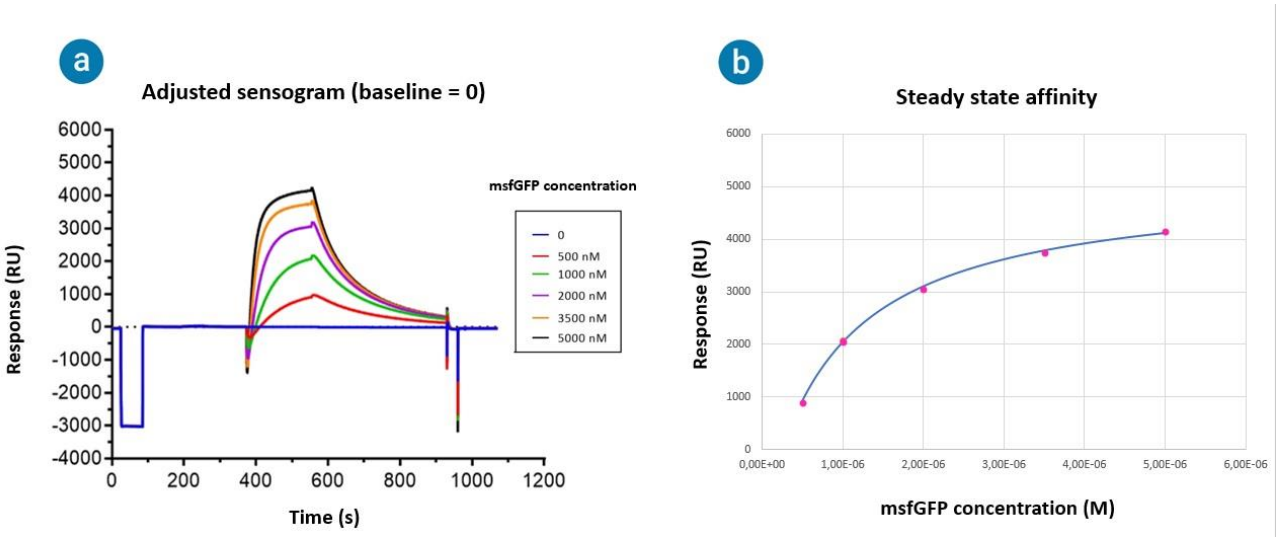

Figure 9. SPR results for binding analysis of ABBA 274-715 and msfGFP (negative control). A) Adjusted sensograms for different concentrations of the analyte; B) Steady state affinity; RU = resonance unit

Similarly as with the MST assays, SPR results show remarkably similar binding behavior for the SH3-tagged analyte and the negative control. Differences of amplitude in the sensograms and steady state affinity plots between the two experiments can be explained by difference in molecular weight caused by the SH3-domain (Table 3).

4.6. Biochemical binding assays with peptides

As a final experiment, I wanted to test if an interaction would occur between the NEDD9 SH3-domain and the proline-rich class II consensus motif that was identified in the ABBA sequence (Figure 5). Surprisingly, MST assays done with the ABBA peptide produced different results for the two fluorescent targets (Figure 10). While the negative control once again resulted in changes of the fluorescence signal and a binding curve, the assay done with msfGFP-SH3 showed seemingly stable fluorescent signals in the capillary scan (Figure 10a). No binding was detected for ABBA 546-550 and msfGFP-SH3 (Figure 10c).

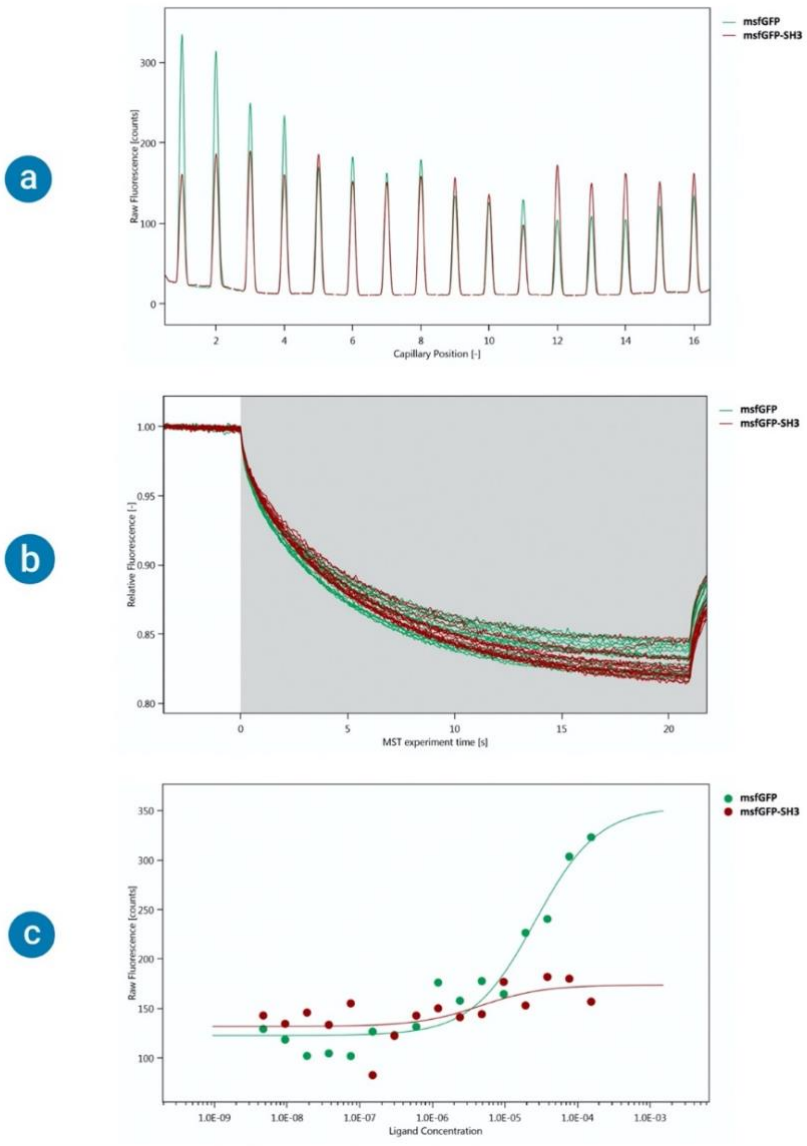

Figure 10. Results from MST binding analyses using ABBA 546-560 peptide as the ligand, and either msfGFP-SH3 or msfGFP as the fluorescent target. A) Capillary scans showing fluorescent target signals in capillaries 1-16. B) MST-traces C) Binding curves plotted using raw fluorescence values.

Finally, an SPR assay was optimized and done with the proline-rich ABBA peptide (546-560) as the analyte, and 6xHis-msfGFP-SH3 as the ligand immobilized on the chip. Similarly as with the MST assay, no binding was detected for the pair (Figure 11).

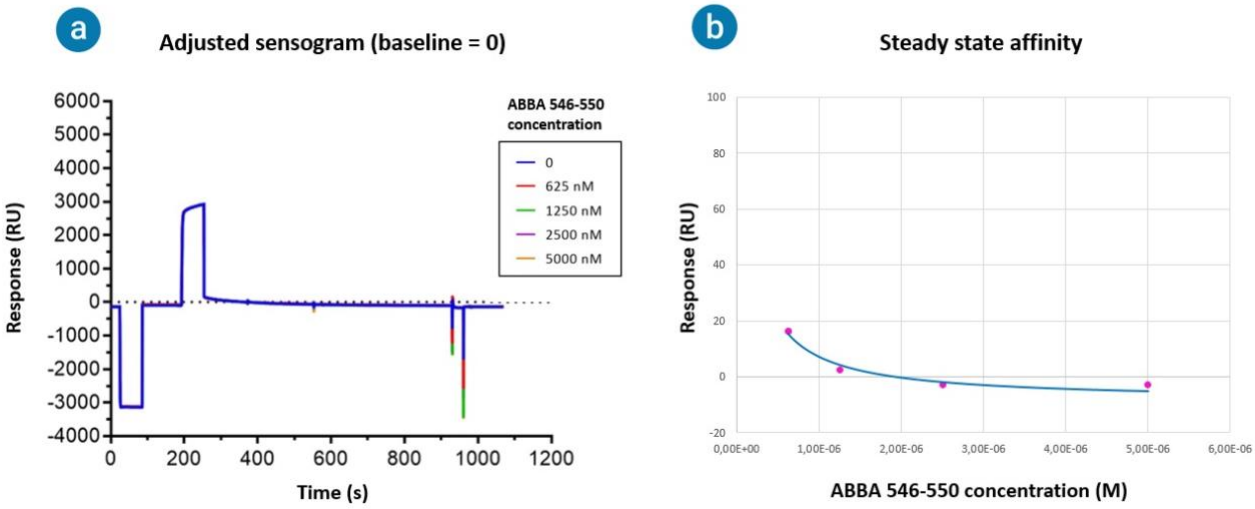

Figure 11. SPR assay results of immobilized 6xHis-msfGFP-SH3 and ABBA 546-560 peptide. A) Adjusted sensograms for different concentrations of the analyte; B) Steady state affinity; RU = resonance unit

5. Discussion

ABBA and NEDD9 have both been formerly identified as enriched proteins in certain radial glial cells during embryonic development. Previous data have indicated an interaction between these two proteins, and also suggested towards their interaction being a significant factor in radial glial cell processes. In my thesis, I aimed to validate the interaction of ABBA and NEDD9 biochemically, and test if it is mediated directly by specific domains of these proteins. I started my thesis work by doing binding assays on endogenous proteins and based on those results moved on to biochemical binding assays with purified constructs representing the domains of interest.

5.1. Co-immunoprecipitation of endogenous proteins

Based on the results from co-immunoprecipitation of endogenous ABBA and NEDD9, it seems that ABBA indeed pulls down NEDD9 from C6 cells, indicating interaction between the two. Interestingly, ABBA seems to preferentially interact with the non-phosphorylated or less phosphorylated (p105) form of NEDD9, due to the lower band at around 100 kDa being more prominent in the ABBA-bound fraction (Figure 4), whereas hyper-phosphorylated NEDD9 (p115) is a clearly more abundant band in the lysate fraction.

Although factors influencing the NEDD9 p105/p115 ratio in cells have not yet been broadly discovered, it is known that both actin cytoskeleton integrity and cell adhesion are contributing processes (Singh et al., 2007). The active hyper-phosphorylated form of NEDD9 is also known to accumulate specifically during the G2/M-phase of the cell cycle (Shagisultanova et al., 2015). Therefore, preferential binding of ABBA to non-phosphorylated NEDD9 indicates that their interaction could occur at a specific point during the cell cycle . This could also be explained by the fact that hyper-phosphorylated NEDD9 is the active form that binds with several other partners, which could prevent its interaction with ABBA. This possible role of phosphorylation in the regulation of NEDD9 interaction with ABBA needs to be confirmed in the future. One approach could be to use mutations targeting the known phosphorylation sites in NEDD9 to inhibit its phosphorylation or dephosphorylation in cells. If the interaction between ABBA and NEDD9 takes place preferentially during a specific cell cycle phase, cell synchronization and collection of cells in

different cell cycle stages could be considered as an approach to validate this in future pull-down assays with the endogenous proteins. Finally, although protease inhibitors were used throughout the co-immunoprecipitation protocol, it is significant to consider that the p115 form of NEDD9 is seen as the main target for degradation, which could possibly affect the results.

Due to a limited supply of primary antibodies, the co-immunoprecipitation experiments were not optimized further in the scope of this thesis work. In the future, it would be important to validate these results with an opposite approach, by using NEDD9 as the primary target in pull-down assays instead of ABBA. I did not test this in my thesis work, since our primary antibody against NEDD9 was monoclonal (Table 1), and if the interaction of ABBA and NEDD9 would cover up the epitope in NEDD9, our antibody would not be able to recognize it. However, based on these preliminary results already, it can be concluded that an interaction likely occurs between ABBA and NEDD9 in C6 cells. Whether this interaction is direct or mediated by other proteins as a part of a larger complex is not known. Thus, it would be relevant to proceed optimizing this method in order to confirm this. Based on the results of the two optimization attempts shown in Figure 4, a good approach would be to repeat the assay using the methods of the first attempt (Figure 4a) with a consistent negative control.

5.2. Biochemical binding assays

Contrary to the co-immunoprecipitation results, further biochemical binding assays did not confirm the physical binding of NEDD9 SH3-domain and C-terminal ABBA. The unexpected initial results from MST assays with C-terminal ABBA and the msfGFP-constructs led to a conclusion, that the fluorescence changes that resulted in what looks like binding curve (Figure 7c), are not in fact binding specific, since after adding detergent to the reactions this phenomenon disappears. However, since addition of detergent even in small concentrations resulted in no binding detected between C-terminal ABBA and msfGFP (data not shown), there was no option to optimize the assays further, with the constructs that had been purified. Due to the inconclusive results from MST assays, I wanted to further test the binding of the purified constructs with SPR, where fluorescence is not a contributing factor in the binding detection method. Surprisingly SPR results confirmed, that there indeed is a binding occurring between the partners, but that it is not specific to the SH3-domain.

Estimated K_D-values that resulted from the different biochemical binding assays (Table 6) are all within a range of 0,6 - 1,5 µM. In literature, the binding affinity of SH3-domains and canonical proline-rich target sequences (class I and II) is estimated to be within the range of 1-200 µM (Li, 2005). The obtained K_D-values between the empty negative msfGFP-control and the SH3-domain containing construct are consistent in both experimental approaches. Both MST and SPR results show that the empty control seems to bind with a greater affinity to C-terminal ABBA, than the SH3-construct. This is a very surprising and unexpected finding. Non-specific binding mediated either by the 6x-His-affinity tag or msfGFP in the constructs used in these experiments is a possibility, but highly unlikely since these are commonly used tags due to them being considered to have minimal non-specific binding with other proteins. In an attempt to pinpoint the problem of seemingly non-specific binding, BSA was used as a negative ligand control (in place of C-terminal ABBA) in MST assays. This gave a similar result of non-specific binding as with the other constructs, even with a "double-negative" control (BSA + empty msfGFP; data not shown). These results, taken together with the SPR experiments where msfGFP-constructs lacking a 6xHis-tag were used, it would seem that msfGFP in itself is causing these results of unexpected binding. If these experiments were to be repeated in the future, different fluorescent tags should be tried in the MST assays. For SPR experiments, neither partner requires a fluorescent tag, so possibly the SH3-domain (or other domains of the NEDD9 protein) could be purified solely with a 6xHis-affinity tag for these assays.

Using the ABBA 546-560 custom peptide as an alternative partner to test binding with SH3, showed that the canonical class II site that was identified from the ABBA protein sequence (Figure 5), is not binding-specific for the SH3-domain of NEDD9. It is possible that in case the interaction of these two proteins is indeed a direct one, it is carried out by different domains or binding sites than what we predicted here. There could be various other non-consensus binding sites within the C-terminal portion of ABBA, which cannot be predicted directly from the protein sequence. Saksela and Permi (2012) evaluated, that the binding affinity and selectivity mediated by these non-consensus SH3 binding sites could be much greater than for the known Class I and Class II consensus sites and that these non-canonical interactions could make up for a substantial portion of all SH3-domain interactions. Overall, the results from MST and SPR binding assays could not confirm my hypothesis that a direct interaction with ABBA is mediated by the NEDD9 SH3-domain.

Thus, other domains of NEDD9 or additional proteins might be involved in facilitating the potential interaction between these two proteins.

5.3. Concluding remarks and future prospects

Radial glial cells undergo mitotic divisions throughout embryonic cortical development, and their unique division style is a significant factor in healthy cerebral cortex formation. Specifically, their cleavage furrow orientation affecting daughter cell fate as well as their unique migratory behaviors (MST and INM) throughout the cell cycle are known characteristics for these cells. These processes require distinct molecular mechanisms, which are still largely unknown. Previous data have shown, that ABBA and NEDD9 proteins are prominent in radial glial cells during certain embryonic stages, and their interaction could be a key contributor in correct cortical development. ABBA has a known function in the regulation of plasma membrane and actin dynamics in radial glial like cells, while NEDD9 is extensively regulated throughout the cell cycle, to ensure that cells are able to progress from mitosis to cytokinesis. Together these known biological functions of ABBA and NEDD9 as well as findings presented here regarding their potential interaction, raise questions about the exact roles of these proteins in radial glial cells . Their interaction could be limited to a distinct phase of the cell cycle, and it will be important to conduct further interaction and colocalization studies in order to dissect this specific biological role in the future, as well as see whether its disruption leads to defects in cortical development.

Although the results from this thesis work, notably from the different biochemical binding assays, were disappointing and did not prove the original hypothesis of direct interaction to be correct, they have shed new light on how this research topic could be approached in the future. One possibility is that the interaction of ABBA and NEDD9 is not in fact direct between the two proteins, but requires additional binding partners which all together form a functional complex. These additional factors could be identified for example by subjecting the eluates from ABBA and NEDD9 immunoprecipitations to mass spectrometry and trying to identify common interactors. However, the possibility of a direct interaction should not be dismissed, and this topic requires further research. The physical interaction of these proteins could possibly be studied between different domains, than what have been focused on in this thesis. It will also be interesting to see, if new patient mutations in these genes are discovered in the future in the context of cortical

malformations, and what kind of new information that will provide about their biological roles and possibly important interaction sites.

Acknowledgements

Firstly, I want to thank my supervisor Juha Saarikangas for accepting me to be a part of his talented group of scientists and giving me the opportunity of working on such an interesting thesis topic. I greatly appreciate him always keeping his office door open, for when advice and guidance was needed. A special thank you goes to our collaborators in France, Claudio Rivera and Aurelie Carabalona, who have given valuable insights at various stages of my thesis work and shared with us their own exciting findings. I would also like to thank Pekka Lappalainen and his group for providing me with the necessary plasmids, antibodies and other materials for my experiments. Additionally I want to thank Maria Aatonen from the Biomolecular Interactions unit for teaching me the difficult methods that were necessary to master for completing my thesis work. Last but not least, I am truly grateful for my wonderful fellow lab-mates, whose company and support during this thesis work has been beyond important.

References

Alazami, A., Patel, N., Shamseldin, H., Anazi, S., Al-Dosari, M., Alzahrani, F., Hijazi, H., Alshammari, M., Aldahmesh, M., Salih, M., Faqeih, E., Alhashem, A., Bashiri, F., Al-Owain, M., Kentab, A., Sogaty, S., Al Tala, S., Temsah, M., Tulbah, M., Aljelaify, R., Alshahwan, S., Seidahmed, M., Alhadid, A., Aldhalaan, H., AlQallaf, F., Kurdi, W., Alfadhel, M., Babay, Z., Alsogheer, M., Kaya, N., Al-Hassnan, Z., Abdel-Salam, G.H., Al-Sannaa, N., Al Mutairi, F., El Khashab, H., Bohlega, S., Jia, X., Nguyen, H., Hammami, R., Adly, N., Mohamed, J., Abdulwahab, F., Ibrahim, N., Naim, E., Al-Younes, B., Meyer, B., Hashem, M., Shaheen, R., Xiong, Y., Abouelhoda, M., Aldeeri, A., Monies, D. & Alkuraya, F. 2015, Accelerating novel candidate gene discovery in neurogenetic disorders via whole-exome sequencing of prescreened multiplex consanguineous families, *Cell Reports*, **10**(2), p. 148-161.

Aquino, J.B., Lallemend, F., Marmigère, F., Adameyko, I.I., Golemis, E.A. & Ernfors, P. 2009, The retinoic acid inducible Cas-family signaling protein Nedd9 regulates neural crest cell migration by modulating adhesion and actin dynamics, *Neuroscience*, **162**(4), p. 1106-1119.

Aquino, J.B., Marmigère, F., Lallemend, F., Lundgren, T.K., Villar, M.J., Wegner, M. & Ernfors, P. 2008, Differential expression and dynamic changes of murine NEDD9 in progenitor cells of diverse tissues, *Gene Expression Patterns*, **8**(4), p. 217-226.

Beattie, R. & Hippenmeyer, S. 2017, Mechanisms of radial glia progenitor cell lineage progression, *FEBS Letters,* **591**(24), p. 3993-4008.

Borrell, V. 2019, Recent advances in understanding neocortical development [version 1; peer review: awaiting peer review], *F1000Research,* **8**, p. 1791.

Chatzi, C., Zhang, Y., Hendricks, W.D., Chen, Y., Schnell, E., Goodman, R.H. & Westbrook, G.L. 2019, Exercise-induced enhancement of synaptic function triggered by the inverse BAR protein, Mtss1L, *eLife,* **8**, p. e45920.

Chou, F., Li, R. & Wang, P. 2018, Molecular components and polarity of radial glial cells during cerebral cortex development, *Cellular and Molecular Life Sciences,* **75**(6), p. 1027-1041.

Dadke, D., Jarnik, M., Pugacheva, E.N., Singh, M.K. & Golemis, E.A. 2006, Deregulation of HEF1 impairs M-phase progression by disrupting the RhoA activation cycle, *Molecular Biology of the Cell,* **17**(3), p. 1204-1217.

Desikan, R.S. & Barkovich, A.J. 2016, Malformations of cortical development, *Annals of Neurology*, **80**(6), p. 797-810.

Hansen, D.V., Lui, J.H., Parker, P.R.L. & Kriegstein, A.R. 2010, Neurogenic radial glia in the outer subventricular zone of human neocortex, *Nature,* **464**(7288), p. 554-561.

Jinnou, H., Sawada, M., Kawase, K., Kaneko, N., Herranz-Pérez, V., Miyamoto, T., Kawaue, T., Miyata, T., Tabata, Y., Akaike, T., García-Verdugo, J.M., Ajioka, I., Saitoh, S. & Sawamoto, K. 2018, Radial glial fibers promote neuronal migration and functional recovery after neonatal brain injury, *Cell Stem Cell,* **22**(1), p. 128-137.e9.

Knutson, D.C., Mitzey, A.M., Talton, L.E. & Clagett-Dame, M. 2015, Mice null for NEDD9 (HEF1) display extensive hippocampal dendritic spine loss and cognitive impairment, *Brain Research,* **1632**, p. 141-155.

Kumar, S., Tomooka, Y. & Noda, M. 1992, Identification of a set of genes with developmentally down-regulated expression in the mouse brain, *Biochemical and Biophysical Research Communications*, **185**(3), p. 1155-1161.

Kurochkina, N. & Guha, U. 2013, SH3 domains: modules of protein–protein interactions, *Biophysical Reviews*, **5**(1), p. 29-39.

LaMonica, B.E., Lui, J.H., Hansen, D.V. & Kriegstein, A.R. 2013, Mitotic spindle orientation predicts outer radial glial cell generation in human neocortex, *Nature communications,* **4**(1), p. 1665.

Li, S.S. 2005, Specificity and versatility of SH3 and other proline-recognition domains: structural basis and implications for cellular signal transduction, *The Biochemical Journal,* **390**(Pt 3), p. 641-653.

Lui, J., Hansen, D. & Kriegstein, A. 2011, Development and evolution of the human neocortex, *Cell*, **146**(1), p. 18-36.

Ohba, T., Ishino, M., Aoto, H. & Sasaki, T. 1998, Dot Far-Western Blot analysis of relative binding affinities of the Src Homology 3 domains of Efs and its related proteins, *Analytical Biochemistry*, **262**(2), p. 185-192.

Ostrem, B., Di Lullo, E. & Kriegstein, A. 2016, oRGs and mitotic somal translocation — a role in development and disease, *Current Opinion in Neurobiology,* **42**, p. 61-67.

Ostrem, B.L., Lui, J., Gertz, C. & Kriegstein, A. 2014, Control of outer radial glial stem cell mitosis in the human brain, *Cell Reports,* **8**(3), p. 656-664.

Pugacheva, E.N. & Golemis, E.A. 2005, The focal adhesion scaffolding protein HEF1 regulates activation of the Aurora-A and Nek2 kinases at the centrosome, *Nature Cell Biology*, **7**(10), p. 937-946.

Pugacheva, E.N. & Golemis, E.A. 2006, HEF1-Aurora A interactions: Points of dialog between the cell cycle and cell attachment signaling networks, *Cell Cycle*, **5**(4), p. 384-391.

Reghunath, A. & Ghasi, R.G. 2020, A journey through formation and malformations of the neo-cortex, *Child's Nervous System*, **36**(1), p. 27-38.

Saarikangas, J., Hakanen, J., Mattila, P.K., Grumet, M., Salminen, M. & Lappalainen, P. 2008, ABBA regulates plasma-membrane and actin dynamics to promote radial glia extension, *Journal of Cell Science,* **121**(9), p. 1444-1454.

Saarikangas, J., Zhao, H., Pykäläinen, A., Laurinmäki, P., Mattila, P.K., Kinnunen, P.K.J., Butcher, S.J., & Lappalainen, P. 2009, Molecular mechanisms of membrane deformation by I-BAR domain proteins, *Current Biology*, **19**(2), p. 95-107.

Saksela, K. & Permi, P. 2012, SH3 domain ligand binding: What's the consensus and where's the specificity? *FEBS Letters,* **586**(17), p. 2609-2614.

Sasaki, T., Iwata, S., Okano, H.J., Urasaki, Y., Hamada, J., Tanaka, H., Dang, N.H., Okano, H. & Morimoto, C. 2005, Nedd9 Protein, a Cas-L homologue, is upregulated after transient global ischemia in rats: possible involvement of Nedd9 in the differentiation of neurons after ischemia, *Stroke*, **36**(11), p. 2457-2462.

Shagisultanova, E., Gaponova, A.V., Gabbasov, R., Nicolas, E. & Golemis, E.A. 2015, Preclinical and clinical studies of the NEDD9 scaffold protein in cancer and other diseases, *Gene,* **567**(1), p. 1-11.

Singh, M., Cowell, L., Seo, S., O'Neill, G. & Golemis, E. 2007, Molecular basis for HEF1/NEDD9/Cas-L action as a multifunctional co-ordinator of invasion, apoptosis and cell cycle, *Cell Biochemistry and Biophysics,* **48**(1), p. 54-72.

Stanishneva-Konovalova, T.B., Derkacheva, N.I., Polevova, S.V. & Sokolova, O.S. 2016, The role of BAR domain proteins in the regulation of membrane dynamics, *Acta naturae,* **8**(4), p. 60-69.

Tikhmyanova, N., Little, J. & Golemis, E. 2010, CAS proteins in normal and pathological cell growth control, *Cellular and Molecular Life Sciences,* **67**(7), p. 1025-1048.

Vogel, T., Ahrens, S., Büttner, N. & Krieglstein, K. 2010, Transforming Growth Factor β promotes neuronal cell fate of mouse cortical and hippocampal progenitors in vitro and in vivo: Identification of Nedd9 as an essential signaling component, *Cerebral Cortex*, **20**(3), p. 661-671.

Zeng, X., Luo, X., Wang, S. & Zhan, X. 2013, Fibronectin-mediated cell spreading requires ABBA-Rac1 signaling, *Journal of Cellular Biochemistry*, 114, p. 773-781.

Zhang, S. & Wu, L. 2015, Roles of neural precursor cell expressed, developmentally downregulated 9 in tumor-associated cellular processes (Review), *Molecular Medicine Reports,* **12**(5), p. 6415-6421.

Zhao, H., Pykäläinen, A. & Lappalainen, P. 2010, I-BAR domain proteins: linking actin and plasma membrane dynamics, *Current Opinion in Cell Biology,* **23**(1), p. 14-21.

Zheng, D., Niu, S., Yu, D., Zhan, X.H., Zeng, X., Cui, B., Chen, Y., Yoon, J., Martin, S.S., Lu, X. & Zhan, X. 2010, Abba promotes PDGF-mediated membrane ruffling through activation of the small GTPase Rac1, *Biochemical and Biophysical Research Communications,* **401**(4), p. 527-532.